

This is a repository copy of  $\beta$  -delayed fission of Am 230.

White Rose Research Online URL for this paper:

<https://eprints.whiterose.ac.uk/id/eprint/122892/>

Version: Accepted Version

---

**Article:**

Wilson, G. L., Takeyama, M., Andreyev, A. N. orcid.org/0000-0003-2828-0262 et al. (18 more authors) (2017)  $\beta$  -delayed fission of Am 230. Physical Review C - Nuclear Physics. 044315. ISSN: 2469-9993

<https://doi.org/10.1103/PhysRevC.96.044315>

---

**Reuse**

Items deposited in White Rose Research Online are protected by copyright, with all rights reserved unless indicated otherwise. They may be downloaded and/or printed for private study, or other acts as permitted by national copyright laws. The publisher or other rights holders may allow further reproduction and re-use of the full text version. This is indicated by the licence information on the White Rose Research Online record for the item.

**Takedown**

If you consider content in White Rose Research Online to be in breach of UK law, please notify us by emailing [eprints@whiterose.ac.uk](mailto:eprints@whiterose.ac.uk) including the URL of the record and the reason for the withdrawal request.

# $\beta$ -delayed fission of $^{230}\text{Am}$

G. L. Wilson,<sup>1,2</sup> M. Takeyama,<sup>3,4</sup> A. N. Andreyev,<sup>1,5,6</sup> B. Andel,<sup>7</sup> S. Antalic,<sup>7</sup> W. N. Catford,<sup>8</sup> L. Ghys,<sup>9,10</sup>  
H. Haba,<sup>3</sup> F. P. Heßberger,<sup>11,12</sup> M. Huang,<sup>3</sup> D. Kaji,<sup>3</sup> Z. Kalaninova,<sup>7,13</sup> K. Morimoto,<sup>3</sup> K. Morita,<sup>3,14</sup>  
M. Murakami,<sup>3,15</sup> K. Nishio,<sup>5</sup> R. Orlandi,<sup>5</sup> A. G. Smith,<sup>16</sup> K. Tanaka,<sup>3,17</sup> Y. Wakabayashi,<sup>3</sup> and S. Yamaki<sup>3,18</sup>

<sup>1</sup>*Department of Physics, University of York, York, YO10 5DD, UK*

<sup>2</sup>*Department of Physics and Applied Physics, University of Massachusetts Lowell, Lowell, MA 01854, United States*

<sup>3</sup>*Nishina Center for Accelerator-Based Science, RIKEN, Wako, Saitama 351-01, Japan*

<sup>4</sup>*Department of Physics, Yamagata University, Yamagata 990-8560, Japan*

<sup>5</sup>*Advanced Science Research Center, Japan Atomic Energy Agency, Tokai, Ibaraki, 319-1195, Japan*

<sup>6</sup>*ISOLDE, CERN, Geneva CH-1211, Switzerland*

<sup>7</sup>*Department of Nuclear Physics and Biophysics,*

*Comenius University in Bratislava, 84248 Bratislava, Slovakia*

<sup>8</sup>*Department of Physics, University of Surrey, Guildford, Surrey, GU2 7XH, UK*

<sup>9</sup>*Instituut voor Kern- en Stralingsfysica, University of Leuven, Celestijnenlaan 200 D, B-3001 Leuven, Belgium*

<sup>10</sup>*Belgian Nuclear Research Center SCK•CEN, Boeretang 200, B-2400 Mol, Belgium*

<sup>11</sup>*Gesellschaft für Schwerionenforschung Darmstadt, Postfach 110541, 6100 Darmstadt, Germany*

<sup>12</sup>*Helmholtz Institut Mainz, 5099 Mainz, Germany*

<sup>13</sup>*Laboratory of Nuclear Problems, JINR, 141980 Dubna, Russia*

<sup>14</sup>*Department of Physics, Kyusyu University, Motooka, Fukuoka, 819-0395, Japan*

<sup>15</sup>*Department of Chemistry, Niigata University, Niigata 950-2181, Japan*

<sup>16</sup>*School of Physics and Astronomy, University of Manchester, Manchester, M13 9PL, UK*

<sup>17</sup>*Faculty of Science and Technology, Tokyo University of Science, Noda, Chiba 278-8510, Japan*

<sup>18</sup>*Department of Physics, Saitama University, Saitama 338-8570, Japan*

(Dated: September 7, 2017)

The exotic decay process of beta-delayed fission ( $\beta\text{DF}$ ) has been studied in the neutron-deficient isotope  $^{230}\text{Am}$ . The  $^{230}\text{Am}$  nuclei were produced in the complete fusion reaction  $^{207}\text{Pb}(^{27}\text{Al}, 4n)^{230}\text{Am}$  and separated by using the GARIS gas-filled recoil separator. A lower limit for the  $\beta\text{DF}$  probability  $P_{\beta\text{DF}}(^{230}\text{Am}) > 0.24$  was deduced, which so far is the highest value among all known  $\beta\text{DF}$  nuclei. The systematics of  $\beta\text{DF}$  in the region of  $^{230}\text{Am}$  will be discussed.

## I. INTRODUCTION

Beta-delayed fission ( $\beta\text{DF}$ ) is a rare two-step nuclear-decay process in which the parent nuclide first undergoes  $\beta$  decay ( $\beta^+$ /EC or  $\beta^-$ ) populating excited states in the daughter nucleus. If the excitation energy  $E^*$  of the populated states is comparable to, or even higher than the fission barrier height  $B_f$  of the daughter nuclide, then fission may happen instantaneously in competition with gamma and/or particle emission. The observed half-life behaviour of fission events in  $\beta\text{DF}$  is determined by the half-life of the feeding  $\beta$ -decaying parent nucleus. Up to now, 28  $\beta\text{DF}$  nuclides are known, all of them being odd-odd, see the references in the recent review [1] and the study of  $^{240}\text{Es}$ ,  $^{236}\text{Bk}$  in [2]. An important experimental quantity is the  $\beta\text{DF}$  probability, which is defined as the ratio of the number of  $\beta\text{DF}$  decays,  $N_{\beta\text{DF}}$ , to the number of  $\beta$  decays,  $N_\beta$ , of the parent nuclide:

$$P_{\beta\text{DF}} = \frac{N_{\beta\text{DF}}}{N_\beta}. \quad (1)$$

Beta-delayed fission was discovered in the neutron-deficient isotopes  $^{232,234}\text{Am}$  in Dubna in 1966 [3]. These nuclides were further studied in more detail in follow-up experiments in Dubna [4], Berkeley [5, 6] and Karlsruhe [7]. Though different experimental techniques and analysis assumptions were used by Kuznetsov *et*

*al.* [4] (Dubna, 1967) and Hall *et al.* [6, 8] (Berkeley, 1990) in their respective studies of  $^{234}\text{Am}$ , very comparable values of  $P_{\beta\text{DF}}(^{234}\text{Am})$  were deduced, see Table I.

The isotope  $^{232}\text{Am}$  was studied in three experiments, which reported three very different  $P_{\beta\text{DF}}$  values, see Table I. The groups from Dubna [3] and Berkeley [5] used the same experimental techniques and assumptions as for their respective studies of  $^{234}\text{Am}$ . However, the Dubna group reported a  $P_{\beta\text{DF}}(^{232}\text{Am})$  value which is 100 times larger than that deduced by the Berkeley group. Furthermore, the Dubna result is  $\sim 5$  times higher than a measurement undertaken by Habs *et al.* in Karlsruhe in 1978 [7]. The reason for such a large difference between three measurements of  $P_{\beta\text{DF}}(^{232}\text{Am})$  is as yet unknown. It should be noted that the value obtained by the Berkeley group [5], being the lowest of three, is thought to be the most accurate, see discussion in [1]. However, for the consistency of the discussion, all three values of  $P_{\beta\text{DF}}(^{232}\text{Am})$  have been plotted in Fig. 1, which shows the measured  $P_{\beta\text{DF}}$  values as a function of the  $Q_{\text{EC}}(\text{Parent}) - B_f(\text{Daughter})$  difference. Here, 13 nuclides with ‘reliably measured’  $P_{\beta\text{DF}}$  values, as evaluated by Ref. [1], were used, with an addition of two recently reported values for  $^{240}\text{Es}$  and  $^{236}\text{Bk}$  from [2]. Figure 1 shows an overall linear dependence of  $\log(P_{\beta\text{DF}})$  on the  $Q_{\text{EC}}(\text{Parent}) - B_f(\text{Daughter})$  difference. However, a caveat should be mentioned here that the plots of logarithmic  $P_{\beta\text{DF}}$  values (and the partial  $\beta\text{DF}$  half-life values

EC/ $\beta^+$ decay	Parent $Q_{EC}$ (MeV) [9]	Daughter $B_f$ (MeV) [10]	$Q_{EC} - B_f$ (MeV)	EC/ $\beta^+$ branch (%)	$T_{1/2}$ (precursor) (min)	$P_{\beta DF}$
$^{234}\text{Am} \rightarrow ^{234}\text{Pu}$	4.12	3.83	0.29	$\sim 100$ [6]	2.32(8) [6]	$\sim 6.95 \times 10^{-5}$ , Dubna [4] $6.6(18) \times 10^{-5}$ , Berkeley [6]
$^{232}\text{Am} \rightarrow ^{232}\text{Pu}$	4.88	3.23	1.65	$\sim 97$ [5]	1.31(4) [5]	$6.96 \times 10^{-2}$ , Dubna [3] $(1.3_{-0.8}^{+4}) \times 10^{-2}$ , Karlsruhe [7] $6.9(10) \times 10^{-4}$ , Berkeley [5]
$^{230}\text{Am} \rightarrow ^{230}\text{Pu}$	5.68	3.07	2.61	$\sim 100$	0.52, this work*	$>0.24$ , this work

TABLE I. Calculated  $Q_{EC}$  values for electron capture and fission barrier heights,  $B_f$ , for  $\beta DF$  of  $^{230,232,234}\text{Am}$  (from Ref. [9] and [10], respectively). Literature  $P_{\beta DF}$  values for  $^{232,234}\text{Am}$  and our experimental lower limit for  $^{230}\text{Am}$  are given in the last column. \*The weighted average of measurements from this work and GARIS [11], see text.

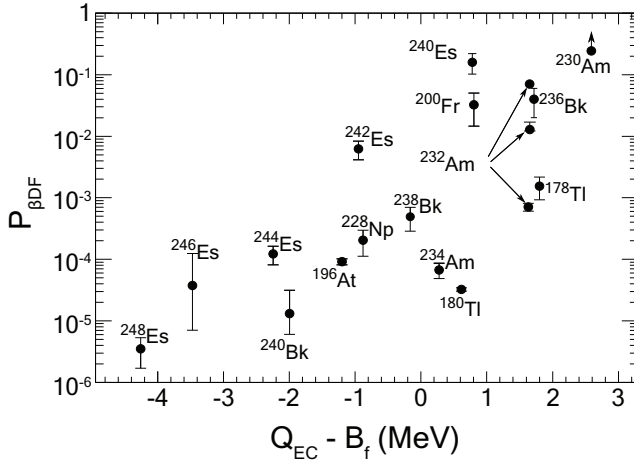


FIG. 1. Experimental  $P_{\beta DF}$  values as a function of the  $Q_{EC}(\text{Parent})-B_f(\text{Daughter})$  difference. Calculated  $Q_{EC}$  and  $B_f$  values are taken from Ref. [9, 10], using the Finite-Range Droplet Model (FRDM) and the Finite-Range Liquid Drop Model (FRLDM), respectively. Three values of  $P_{\beta DF}$  for  $^{232}\text{Am}$  are presented (see Table I), the value of  $P_{\beta DF}$  for  $^{230}\text{Am}$  is from this work.

$T_{1/2, \beta DF}$ , which can be obtained from  $P_{\beta DF}$ , see [12]) can show somewhat different, but still linear, trends if one uses different models to estimate  $Q_{EC}$  and  $B_f$  values, see the discussion of Fig. 12 in [1] or Fig. 4 of [12].

The very neutron-deficient isotope  $^{230}\text{Am}$  is expected to possess one of the largest differences of  $Q_{EC}(\text{Parent})-B_f(\text{Daughter}) \sim 2.61$  MeV for  $\beta DF$  nuclides, see Table I and Fig. 1. By using the  $P_{\beta DF}$  for  $^{232}\text{Am}$  obtained in Berkeley and extrapolating  $P_{\beta DF}(^{232,234}\text{Am})$  data to  $^{230}\text{Am}$  in Fig. 1, a value of  $P_{\beta DF}(^{230}\text{Am}) \sim 10^{-2}$  ( $\sim 1\%$ ) can be estimated. However, in the case of using the much higher values of  $P_{\beta DF}(^{232}\text{Am})$  from Karlsruhe or Dubna, a much higher extrapolated probability of  $P_{\beta DF}(^{230}\text{Am})$  would be obtained, approaching 100%. Therefore, a measurement of  $P_{\beta DF}(^{230}\text{Am})$  would allow a better insight into the systematics of  $\beta DF$  in this region of extremely neutron-deficient nuclei.

In an earlier experiment at GARIS (coupled to the gas-jet system), aimed at the identification of the new isotope  $^{234}\text{Bk}$  in the reaction  $^{197}\text{Au}(^{40}\text{Ar}, 3n)^{234}\text{Bk}$ , six fission events following  $\alpha$  decays of  $^{234}\text{Bk}$  were reported, and a suggestion was made that these fission events could be due to the  $\beta DF$  of  $^{230}\text{Am}$  [11]. We note that no  $\alpha$  decay of  $^{230}\text{Am}$  was observed in the GARIS study, which allows a first experimental determination of the  $\beta$ -decay branch of  $^{230}\text{Am}$  as  $b_{\beta}(^{230}\text{Am}) > 90\%$ . This estimate is in agreement with a value of  $b_{\beta}(^{230}\text{Am}) \sim 75\%$ , which was calculated using a predicted partial  $\beta$ -decay half-life of 42.3 s from Möller *et al.* [13] and the total half-life of  $T_{1/2}(^{230}\text{Am}) = 32_{-9}^{+22}$  s, determined from six fission events in Ref. [11]. A particular limitation of this work with respect to fission measurements was that due to the experimental method used, no fission fragment energies could actually be measured, and only ‘high energy’ saturated signals were registered for events above 20 MeV, see details in Ref. [11].

Therefore, we decided to undertake a dedicated experiment to study possible  $\beta DF$  of  $^{230}\text{Am}$  by directly producing this isotope in the complete fusion reaction  $^{207}\text{Pb}(^{27}\text{Al}, 4n)^{230}\text{Am}$ . Due to the direct production (rather than via the  $\alpha$  decay of  $^{234}\text{Bk}$ ) a higher production cross-section could be expected.

## II. EXPERIMENTAL SETUP

In the present experiment, a beam of 145-MeV  $^{27}\text{Al}$  ions was delivered by RILAC, at RIKEN. The beam was provided at an intensity of 0.5-1.5 pμA (where 1 pμA =  $6.24 \times 10^{12}$  particles/s) for 6 days. Three modes of beam pulsing were used, with the ‘beam ON/beam OFF’ intervals of 40 s/40 s, 5 s/5 s and 20 s/60 s. These modes represent 20%, 31% and 49% of the data collection periods, respectively.

The rotating  $^{207}\text{Pb}$  target was installed in the gas-filled target chamber of the GARIS separator with the helium gas at a pressure of 0.5 mbar. The use of a differential pumping system in front of the target chamber avoided

the need of an extra window to separate the high vacuum of the beam-transport system and the helium-gas filled separator. This allowed the use of the higher beam intensities and to reduce the  $^{27}\text{Al}$  beam scattering. Sixteen  $^{207}\text{Pb}$  target segments were mounted onto a rotating-wheel target frame. The thickness of the targets ranged from 340 to 430  $\mu\text{g}/\text{cm}^2$ , the carbon target backing had a thickness of 60  $\mu\text{g}/\text{cm}^2$ . The target wheel rotated at 3600 rpm.

The reaction products of interest recoiling out of the target (hereafter called ‘recoils’) were separated by GARIS from the primary beam and unwanted background products such as scattered target recoils and transfer reaction products. GARIS consists of four magnets in  $D1-Q1-Q2-D2$  configuration (further details provided in Ref. [14]), with  $B\rho$  set to 1.8 Tm in this work. The detection chamber, situated at the focal plane of GARIS at a distance of 6.16 m from the target, was separated from the gas-filled volume of GARIS by a 0.5- $\mu\text{m}$  thick Mylar foil and evacuated down to  $10^{-6}$  mbar.

For the measurements in the 40/40 s and 5/5 s ‘beam ON/beam OFF’ modes, the separated recoils passed two time of flight (TOF) detectors, each consisting of a 0.5- $\mu\text{m}$  thick mylar foil with an effective area of 78 mm in diameter. Signals were obtained from secondary electrons which are emitted when ions pass through the foils, and are collected by microchannel plates. After passing these TOF detectors, recoils were implanted into a position-sensitive silicon detector (PSD), with a total area of  $58 \times 58 \text{ mm}^2$  divided in 16 longitudinal strips. Upstream of the PSD, four unsegmented silicon detectors, also with an active area of  $58 \times 58 \text{ mm}^2$ , were mounted in a ‘box’ configuration. These detectors, hereafter called ‘BOX detectors’, were used to measure the energies of  $\alpha$  particles and fission fragments escaping from the PSD in the backward direction. The signals from the TOF detectors were used to distinguish decay events in the PSD and the implantation events, by requiring an anticoincidence condition between the signals from the PSD and from at least one of the TOF detectors. The same PSD-BOX detection system was exploited in the measurements with the 20/60 s beam pulsing mode, but no TOF detectors were used. The combined PSD-BOX detection efficiency for  $\alpha$  particles or double-fold fission events was  $\epsilon_\alpha = \epsilon(\text{double-fold FF}) = 85\%$  [14].

The energy calibration of the PSD and of the BOX detectors in the region of fission fragments with energies of up to  $\sim 150$  MeV (see below) relied on the extrapolation of the calibration based on  $\alpha$  decays of  $^{211}\text{At}$  and  $^{211}\text{Po}$  isotopes (with energy 5869.5(22) and 7450.3(5) keV, respectively [15]), produced in the same reaction after a few-nucleon transfer on the  $^{207}\text{Pb}$  target. The energy of the initial  $^{27}\text{Al}$  beam leaking through GARIS with low intensity was also used as a calibration point, after accounting for the energy losses in the target, TOF and other foils. This procedure does not account for the pulse-height defect for fission fragments being measured by the silicon PSD and BOX detectors, this issue will be

discussed further in the text. A typical energy resolution for  $\alpha$  particles measured only by PSD varied between the strips in the range of 34 to 105 keV (FWHM) at 7450 keV.

### III. EXPERIMENTAL RESULTS

#### A. Beta-delayed fission of $^{230}\text{Am}$

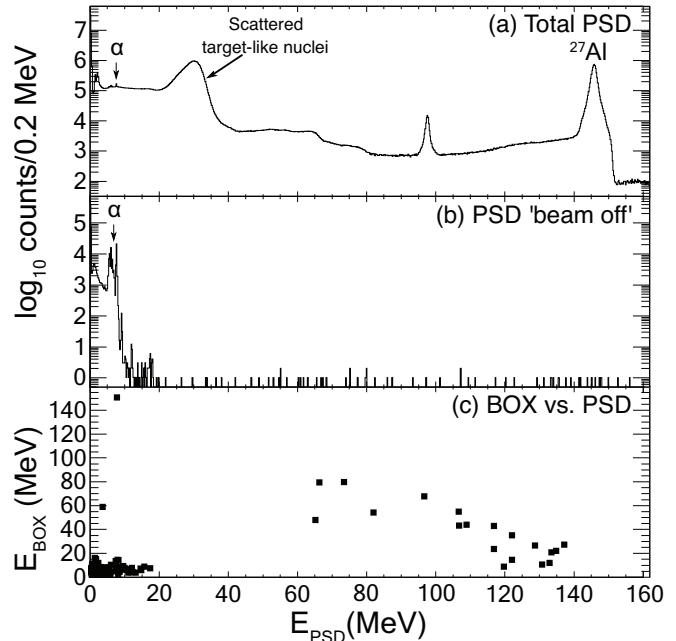


FIG. 2. (a) Total energy spectrum in the PSD in the reaction  $^{207}\text{Pb}(^{27}\text{Al},4n)^{230}\text{Am}$ . The peaks are described in the text. (b) The same as (a), but within ‘beam off’ interval (either 40 s, 5 s or 60 s, see text), and with a TOF anticoincidence condition when the TOF detectors were used. (c) Two dimensional BOX vs. PSD spectrum, with the same gating conditions as (b). A threshold condition, that  $E_{\text{BOX}} > 2$  MeV and  $E_{\text{PSD}} > 2$  MeV, has been applied.

Figure 2(a) shows the total energy spectrum of all events registered in the PSD in the reaction  $^{207}\text{Pb}(^{27}\text{Al},4n)^{230}\text{Am}$  at the beam energy of  $E(^{27}\text{Al}) = 145$  MeV in front of the target. A few groups of events can be distinguished in the spectrum. The highest energy group corresponds to the ‘full’ energy  $^{27}\text{Al}$  beam projectiles ‘leaking’ through GARIS with low intensity. The broad structure around and below  $\sim 30$  MeV corresponds to the scattered target-like nuclei and target-like transfer products. The broadly-distributed structure with the energy in the range of (40-140) MeV is due to lower-energy scattered  $^{27}\text{Al}$  ions. The  $\alpha$  decays of the implanted recoil nuclei and their daughters are seen at  $E_{\text{PSD}} < 9$  MeV. The reason for the low-intensity peak at  $\sim 95$  MeV is not clear, most probably it could be some beam contaminant with a similar A/q ratio as of the  $^{27}\text{Al}$  beam.

Figure 2(b) shows the same spectrum as Fig. 2(a), but registered only during the ‘beam off’ time intervals,



which corresponds to either 40 s, 5 s or 60 s, depending on the mode of beam pulsing used. An extra 5 ms is excluded from the start of the ‘beam off’ interval, to further suppress beam and beam-like products to be registered in the PSD after the beam is switched off. An anticoincidence condition between the signals from the PSD and from at least one of the TOF detectors was additionally required for the data collected in the 40 s and 5 s ‘beam off’ modes, when the TOF detectors were still exploited. Therefore only decay events should be present in this spectrum. Indeed, the beam and recoil/transfer product peaks disappear, but a number of counts above 20 MeV are still present.

Here we note that we are aware about a small contamination of the GARIS target chamber with the  $^{248}\text{Cm}$  target material, used in some of the previous long-running experiments aimed at the production of superheavy elements.  $^{248}\text{Cm}$  is a long-lived ( $T_{1/2} = 3.5 \times 10^5$  y) isotope with a spontaneous fission branching ratio of  $b_{\text{SF}} = 8.39\%$ . The total kinetic energy release for fission fragments is  $\text{TKE}(^{248}\text{Cm}) = 182.2$  MeV, with the most probable energies for light and heavy mass peaks of 103.4 and 78.7 MeV, respectively [16]. The fission fragments from  $^{248}\text{Cm}$  can pass through GARIS with some probability and be registered in the PSD as *single-fold* events, producing some of the high-energy events in the region above 20 MeV and up to  $\sim 100$  MeV in Fig. 2(b). To quantify this, two dedicated background measurements were performed with no beam on the target. In the first measurement, the valve between the target chamber and GARIS was closed, thus no fission fragments from  $^{248}\text{Cm}$  could reach the PSD. In this mode, within 215 hours of measurements, a single double-fold event with energy of  $E_{\text{PSD}} = 18$  MeV,  $E_{\text{BOX}} = 43$  MeV was observed. In the second measurement, the valve between the target chamber and GARIS was open, allowing  $^{248}\text{Cm}$  fission fragments to pass through GARIS and to be registered in PSD. In this mode, within 55 hours of measurements, 81 single events in the energy range of  $E_{\text{PSD}} = 20 - 100$  MeV were observed, with no events above 100 MeV. Based on the above data, we can conclude that the region of 20 – 100 MeV in Fig. 2(b) can contain the fission events from both SF of  $^{248}\text{Cm}$  and from  $\beta\text{DF}$  of  $^{230}\text{Am}$  (see below). In contrast to this, no events from  $^{248}\text{Cm}$  should be present above 100 MeV in Fig. 2(b), where only the events from  $\beta\text{DF}$  of  $^{230}\text{Am}$  and from any remaining ‘leaked’  $^{27}\text{Al}$  can occur.

Despite the presence of the aforementioned background, the unique distinction between the *single-fold* background fission events due to  $^{248}\text{Cm}$  (also the ‘leaked’  $^{27}\text{Al}$  beam) and the  $\beta\text{DF}$  of  $^{230}\text{Am}$  can be done via the detection of prompt *double-fold* PSD-BOX events with large energy deposition (see below). This method provides an unambiguous selection of fission fragments, emitted back-to-back in the  $\beta\text{DF}$  of  $^{230}\text{Am}$  nuclei implanted in the PSD. The two-dimensional  $E_{\text{BOX}} - E_{\text{PSD}}$  spectrum corresponding to events in Fig. 2(b) is shown in Fig. 2(c). An energy condition of  $E_{\text{BOX}} > 2$  MeV

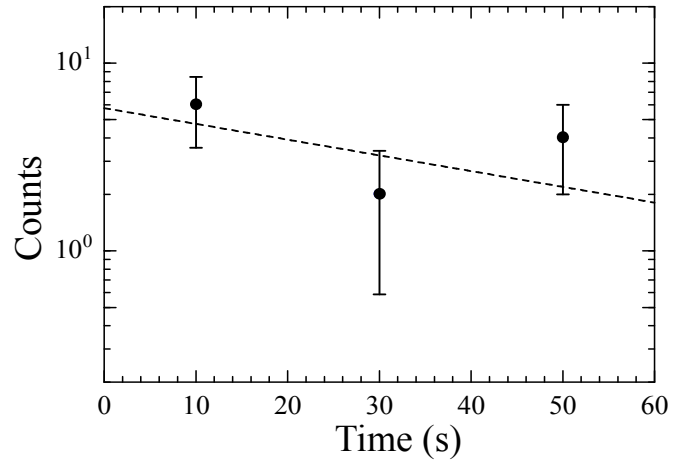


FIG. 3. Time distribution of twelve double-fold fission events collected in the 60 s ‘beam OFF’ time interval of the 20/60 s beam pulsing mode measurements, with an exponential fit shown by a dashed line.

and  $E_{\text{PSD}} > 2$  MeV was applied to eliminate random coincidences with low-energy background events and electronics/detectors noise. A total of 19 double-fold fission events with  $E_{\text{PSD}} > 50$  MeV were detected, which, as shown in Sec. III B, should be attributed to the  $\beta\text{DF}$  of  $^{230}\text{Am}$ .

An estimate of the total kinetic energy release,  $\text{TKE}(^{230}\text{Pu})$ , could be done by summing the measured PSD+BOX energies for these nineteen fission events. In such a way, an ‘apparent’  $\text{TKE}(^{230}\text{Pu}) \sim 146$  MeV was obtained. However, the detectors’ calibration procedure used (based on  $\alpha$  particles and  $^{27}\text{Al}$  beam) does not account for the pulse-height defect of fission fragments in the silicon detectors and also their energy loss in the dead layers. As shown in the previous work at the SHIP velocity filter (Ref. [17], for example), this effect can be as high as 20 to 50 MeV and depends on the implantation depth [18, 19]. In the present study a similar calibration procedure was used, based on the measurements of the ‘apparent’ TKE values for the fission fragments from the spontaneous fission of  $^{252}\text{No}$  (produced in a separate experiment at GARIS) as a function of the implantation depth and comparing them to the tabulated TKE value [20]. A respective energy correction of 24(14) MeV was deduced in our study, which, after summing up with the ‘apparent’ TKE value mentioned above, resulted in the full value of  $\text{TKE}(^{230}\text{Pu}) = 170(20)$  MeV. This value is  $\sim 10$  MeV lower than the expected value of  $\text{TKE} = 180$  MeV following the Viola systematics [21], but is still in agreement within a rather large uncertainty of our measurement.

To deduce the half-life of  $^{230}\text{Am}$ , the data from the 20/60s ‘beam ON/beam OFF’ measurements were used. Fig. 3 shows the time distribution of 12 double-fold fission events observed within the 60 seconds ‘beam OFF’ interval, together with a fit with an exponential function. The resulting half-life  $T_{1/2}(^{230}\text{Am}) = 36_{-8}^{+15}$  s agrees with

a value of  $T_{1/2} = 32_{-9}^{+22}$  s deduced in Ref. [11], based on 6 observed fission events. By combining the data from both experiments, a value of  $T_{1/2}(^{230}\text{Am}) = 36_{-7}^{+12}$  s was deduced.

A production cross-section of  $\sim 540$  pb was deduced for the production of  $^{230}\text{Am}$  in the reaction channel  $^{207}\text{Pb}(^{27}\text{Al}, 4n)^{230}\text{Am}$  at the beam energy used in this study. A calculated GARIS transmission efficiency of 20% was used to derive this value.

## B. Assignment of fission events to $\beta\text{DF}$ of $^{230}\text{Am}$

First we will discuss the assignment of the 19 observed fission events to  $\beta$ -delayed fission of  $^{230}\text{Am}$  rather than to its spontaneous fission (SF) decay. This was done based on systematics of SF half-lives and hindrance factors, as described, for example, in the reviews by Hoffman *et al.* [22] and by Heßberger [23] and references therein. As shown in Fig. 17 in Ref. [23], spontaneous fission in odd- $A$  nuclides is typically hindered by a large factor of  $10^3 - 10^5$  relative to their even-even neighbours. This hindrance is believed to originate due to the so-called ‘specialization energy’ [24] arising from the spin/parity conservation for the odd nucleon in the fission process. It is furthermore expected that the SF hindrance factors for the odd-odd nuclides can be approximately estimated to be the product of the hindrance factors for the odd-neutron and odd-proton neighbours. Indeed, as reviewed in Refs. [22, 23], hindrance factors in excess of  $10^6$  were reported for a number of spontaneously fissioning odd-odd isotopes in the trans-uranium region.

A qualitative estimate for the expected SF half-life of  $^{230}\text{Am}$  could be done in the following way: the closest even-even nuclide with a known SF decay is  $^{234}\text{Cm}$  [23, 25] which has a half-life of 51(12) s, comparable to that of  $^{230}\text{Am}$ . The evaluated partial SF half-life is  $\sim 1500$  s [23, 25]. By applying a hindrance factor of  $10^6$ , a partial SF half-life of  $\sim 10^9$  s would be deduced for  $^{230}\text{Am}$ , which in turn would result in a negligible SF branch, based on the comparison to the measured half-life of  $^{230}\text{Am}$ .

To further confirm our assignment, we mention that none of the lower- $Z$  elements, which could be potentially produced in any evaporation channel ( $p\alpha n$  or  $\alpha\alpha n$ ) of the reaction used or in any transfer channel on the lead target, has a SF decay with a half-life comparable to our experimental value. Furthermore, the only possible candidate for  $\beta\text{DF}$  with lower- $Z$  value -  $^{228}\text{Np}$  has a  $P_{\beta\text{DF}} = 2.0(9) \times 10^{-4}$  [26], which combined with its strongly reduced production in the  $\alpha 2n$  channel (see next section) excludes this isotope as being the source of the observed  $\beta\text{DF}$  activity in our study. Finally, the fact that the same activity seems to be produced in a different reaction in the earlier experiment at GARIS [11] adds another confirmation to the correctness of our identification.

## C. Evaluation of $P_{\beta\text{DF}}(^{230}\text{Am})$

In our work, the  $P_{\beta\text{DF}}(^{230}\text{Am})$  was deduced from the data collected in the 60 s ‘beam-off’ interval in the 20/60s beam pulsing mode. By definition (see Eq. 1), the  $\beta\text{DF}$  probability for  $^{230}\text{Am}$  can be calculated from:

$$P_{\beta\text{DF}}(^{230}\text{Am}) = \frac{N_{\beta\text{DF}}(^{230}\text{Am})}{N_{\beta}(^{230}\text{Am})} \quad (2)$$

where  $N_{\beta\text{DF}}(^{230}\text{Am}) = 12$  is the number of observed double-fold fission events and  $N_{\beta}(^{230}\text{Am})$  is the number of  $\beta$  decays of  $^{230}\text{Am}$  which occurred in this mode.

The number of  $\beta$  decays of  $^{230}\text{Am}$  cannot be measured directly in our experiment, but by definition it is equal to the sum of the number of  $\beta\text{DF}$  events of  $^{230}\text{Am}$ ,  $N_{\beta\text{DF}}(^{230}\text{Am})$ , and the number of the daughter  $^{230}\text{Pu}$  nuclei,  $N(^{230}\text{Pu})$ , see Eq. 3(a), after proper corrections for respective detection efficiencies and branching ratios, where needed.

$$N_{\beta}(^{230}\text{Am}) = N_{\beta\text{DF}}(^{230}\text{Am}) + N(^{230}\text{Pu}) \quad (a)$$

$$= N_{\beta\text{DF}}(^{230}\text{Am}) + \frac{N_{\alpha}(^{230}\text{Pu})}{b_{\alpha}(^{230}\text{Pu})} \quad (b) \quad (3)$$

$$= N_{\beta\text{DF}}(^{230}\text{Am}) + \frac{N_{\alpha\alpha}(^{230}\text{Pu}-^{226}\text{U})}{b_{\alpha}(^{230}\text{Pu}) \times \epsilon_{\alpha} \times 0.94} \quad (c)$$

The  $N(^{230}\text{Pu})$  value is deduced from the number of observed  $\alpha$  decays of  $^{230}\text{Pu}$ ,  $N_{\alpha}(^{230}\text{Pu})$ , corrected, as shown in Eq. 3(b), for the  $\alpha$ -decay branching ratio  $b_{\alpha}(^{230}\text{Pu})$ . An upper limit for the latter was experimentally and model-independently deduced as  $b_{\alpha}(^{230}\text{Pu}) > 73\%$  in Ref. [25], it will be further used to calculate the value of  $P_{\beta\text{DF}}(^{230}\text{Am})$ . In passing we note that a comparable value of  $b_{\alpha}(^{230}\text{Pu}) = 84\%$  was evaluated in [27] by using the calculated  $\beta$ -decay half-life (no uncertainty was given in the original paper).

In our work, the number  $N_{\alpha}(^{230}\text{Pu})$  was determined by searching for time-position correlated  $\alpha$  decays of  $^{230}\text{Pu}$  with the energy of 7.06 MeV with the known  $\alpha$  decays of its daughter isotope  $^{226}\text{U}$  ( $T_{1/2} = 260(10)$  ms), similar to studies [25, 27, 28]. By exploiting both PSD and BOX detectors (thus also adding up the PSD+BOX signals for the ‘escaping’ particles),  $N_{\alpha\alpha}(^{230}\text{Pu}-^{226}\text{U}) = 22$  correlation chains were observed, marked as group *A* in Fig. 4. This value was then used in Eq. 3(c). The applied energy window for  $\alpha$  decay of  $^{226}\text{U}$  included both the g.s.  $\rightarrow$  g.s. (7.560 MeV, 86(3)%) and g.s.  $\rightarrow 2^+$  ( $^{222}\text{Th}$ ) (7.384 MeV, 14(3)%)  $\alpha$ -decay branches, thus no additional correction was needed. The factor of 0.94 in Eq. 3(c) accounts for the fact that only the correlation interval of 4 half-lives was used for Fig. 4. The factor of  $\epsilon_{\alpha} = 0.85$  accounts for the efficiency of measuring a two-member  $\alpha$ - $\alpha$  correlation chain  $^{230}\text{Pu} \rightarrow ^{226}\text{U}$ . We note that we also observed further correlations to grand-daughter  $^{222}\text{Th}$  ( $E_{\alpha} = 7.98$  MeV,  $T_{1/2} = 2.24$  ms), see e.g. the groups *B* and *C* in Fig. 4. The correlations with the follow-up decays of  $^{218}\text{Ra}$  and  $^{214}\text{Rn}$  were also registered, often leading to higher-energy pile-up events, due to the very short half-lives of these isotopes (25.6  $\mu\text{s}$  and 0.27  $\mu\text{s}$ , respectively),

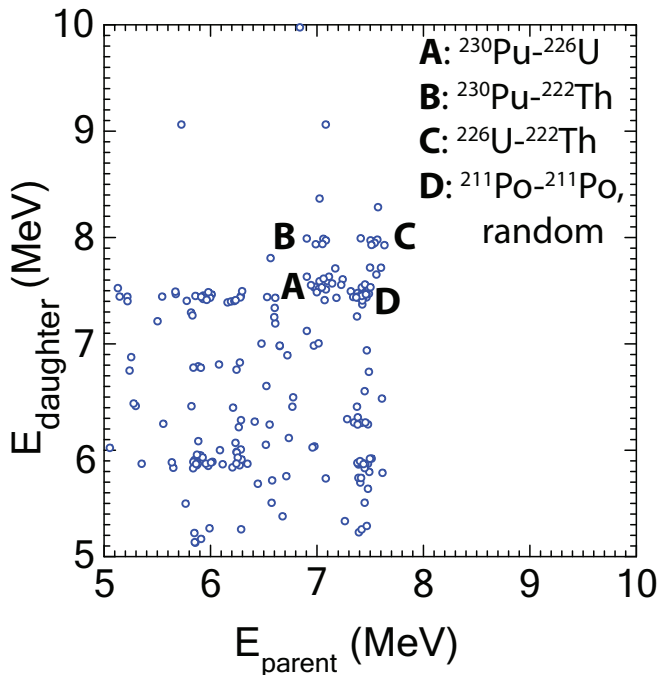


FIG. 4. (Color online)  $\alpha$ - $\alpha$  correlation plot, created for the time interval  $\Delta T(\alpha-\alpha) \leq 1$  s and position window of  $\Delta X(\alpha-\alpha) \leq 2$  mm. The groups originating from the decay of  $^{230}\text{Pu}$  are labeled with symbols A, B, C. Group D represents the random self-correlations between the 7.45 MeV  $\alpha$  decays of  $^{211}\text{Po}$ , abundantly produced in a transfer reaction channel on the  $^{207}\text{Pb}$  target.

see e.g. Fig. 1 of [28]. These events are not shown in Fig. 4 solely for the sake of the simplicity of this figure.

Finally, by combining Eq. 2 and Eq. 3c, the  $P_{\beta DF}(^{230}\text{Am})$  can be calculated as shown in Eq. 4.

$$P_{\beta DF}(^{230}\text{Am}) = \frac{N_{\beta DF}(^{230}\text{Am})}{N_{\beta DF}(^{230}\text{Am}) + \frac{N_{\alpha\alpha}(^{230}\text{Pu}-^{226}\text{U})}{b_{\alpha}(^{230}\text{Pu}) \times \epsilon_{\alpha} \times 0.94}} \quad (4)$$

The application of Eq. 4 relies on the assumption that the direct production of  $^{230}\text{Pu}$  via the  $p3n$  evaporation channel of the  $^{27}\text{Al}+^{207}\text{Pb}$  reaction is about a factor of ten lower than the production of  $^{230}\text{Am}$ , which was estimated by using statistical model code HIVAP [29]. Therefore, most of  $\alpha$ -decay chains of  $^{230}\text{Pu}$  observed in the data should originate after  $^{230}\text{Pu}$  was produced via the  $EC/\beta^+$  decay of  $^{230}\text{Am}$ . Due to this, the  $N_{\alpha\alpha}(^{230}\text{Pu}-^{226}\text{U})$  number was reduced by 10% due to the possible direct production of  $^{230}\text{Pu}$  in the reaction rather than after  $\beta$  decay of  $^{230}\text{Am}$ . Finally, a lower limit of  $P_{\beta DF}(^{230}\text{Am}) > 0.24$  was deduced by using Eq. 4.

We note that no correlated  $\alpha$ -decay chains of the type  $^{230}\text{Am} \rightarrow ^{226}\text{Np}$  were observed, which establishes that the  $\beta$ -decay branch of  $^{230}\text{Am}$  is indeed close to 100% (shown in Table I), in agreement with the estimates given in Section I.

Based on HIVAP calculations we also estimated that

the production cross-section in the  $\alpha xn$  channel is lower by a factor of 5 relative to the  $xn$  channel. Due to a broader angular distribution of products in the  $\alpha xn$  channel, it will be further suppressed by the entrance aperture of GARIS, in comparison to the  $xn$  and  $p xn$  channels.

#### IV. DISCUSSION

The deduced  $P_{\beta DF}(^{230}\text{Am})$  value is the highest so far among all ‘reliably’ measured  $\beta DF$  probabilities, as defined in Ref. [1], see also Fig. 1. With the present measurement, the chain of americium isotopes  $^{230,232,234}\text{Am}$  becomes the third one for which more than two isotopes with the measured  $P_{\beta DF}$  values are known, the other chains being that of five einsteinium nuclides  $^{240,242,244,246,248}\text{Es}$  and of three berkelium isotopes  $^{236,238,240}\text{Bk}$ . This figure also demonstrates that while the three  $P_{\beta DF}$  values for  $^{230,232,234}\text{Am}$  follow the overall increasing trend (as a function of  $Q_{EC}(\text{Parent}) - B_f(\text{Daughter})$  difference) of other nuclides, the  $^{230}\text{Am}$  value is somewhat higher in respect of the linear extrapolation (from a semi-logarithmic plot) from  $^{232,234}\text{Am}$  values. However, as mentioned in Sec. I, a value of  $P_{\beta DF}(^{230}\text{Am}) \sim 0.01$  would be extrapolated if one uses the Berkeley data for  $^{232}\text{Am}$ , while much higher values would result if either Dubna or Karlsruhe data were used. This discrepancy for  $^{230}\text{Am}$  may imply that the Berkeley value for  $^{232}\text{Am}$  could be underestimated, while the measurements by Dubna or Karlsruhe groups could be more accurate.

It is also interesting to note in Fig. 1 the difference in the overall trends of the  $P_{\beta DF}$  values for the chain of the Es and Bk isotopes on the one hand, and of the Am isotopes on the other hand. Indeed, one notices a similar slope for the Es and Bk values. In contrast to this, the Am isotopes demonstrate a very different slope, irrespective of which value is taken for  $^{232}\text{Am}$ . A possible reason for this difference could be the fact that most of data points for the Es and Bk isotopes have negative  $Q_{EC} - B_f$  values, leading to predominantly sub-barrier fission. The latter is mostly determined by the barrier penetrability, thus is expected to have a linear dependence on the  $Q_{EC} - B_f$  difference, while the  $\beta$ -strength function is expected to play less important role. In the case of the Am isotopes, all three measured data points have positive  $Q_{EC} - B_f$  values (at least in the mass model used for Fig. 1), which opens up the possibility of the above-barrier fission, which does not need to follow the linear trend. In this case, also the role of  $\beta$ -strength function might become more important. These considerations show the importance of studying  $\beta DF$  of even lighter isotopes,  $^{228}\text{Am}$ ,  $^{234}\text{Bk}$  and  $^{238}\text{Es}$ , all of which should have large positive  $Q_{EC} - B_f$  differences, and large  $P_{\beta DF}$  probabilities.

Due to the lack of detailed nuclear spectroscopy information on the decay of  $^{230}\text{Am}$ , a discussion of the possible structure of  $^{230}\text{Am}$ , e.g. spin, parity and under-

lying configuration, would be highly tentative at this moment. As a general recommendation, dedicated  $\beta$ -decay studies of the lightest americium isotopes, e.g. by the mass-separator technique used in Refs. [30, 31], should be performed. Such studies have been recently initiated at the mass separator coupled to the tandem at the Japan Atomic Energy Agency (JAEA) at Tokai (Japan) [32].

## V. CONCLUSIONS

The exotic process of  $\beta$ -delayed fission has been studied in the extremely neutron-deficient isotope  $^{230}\text{Am}$ , produced directly in the complete fusion reaction  $^{207}\text{Pb}(^{27}\text{Al}, 4n)^{230}\text{Am}$ . A lower limit for the value of the  $\beta$ DF probability  $P_{\beta DF}(^{230}\text{Am}) > 0.24$  was deduced, which is the highest so far among all known nuclei. The exper-

iment showed the prospects of extending such measurements to even more neutron-deficient isotope  $^{228}\text{Am}$ , in which a value close to 100% would be expected, based on an even larger  $Q_{EC}(\text{Parent}) - B_f(\text{Daughter}) = 3.73 \text{ MeV}$  difference in comparison to  $^{230}\text{Am}$ .

## VI. ACKNOWLEDGMENTS

This experiment was performed at RI Beam Factory operated by RIKEN Nishina Center and CNS, the University of Tokyo. This work has been funded by FWO-Vlaanderen (Belgium), by the Slovak Research and Development Agency (Contract No. APVV-0105-10 and APVV-14-0524) and Slovak Grant Agency VEGA (Contract No. 1/0532/17), by the UK Science and Technology Facilities Council (STFC), and by the Reimei Foundation of JAEA.

- 
- [1] A. N. Andreyev, M. Huyse, P. Van Duppen, *Rev. Mod. Phys.* **85** (2013) 1541–1559. doi:10.1103/RevModPhys.85.1541.
  - [2] J. Konki, J. Khuyagbaatar, J. Uusitalo, P. Greenlees, K. Auranen, H. Badran, M. Block, R. Briselet, D. Cox, M. Dasgupta, A. D. Nitto, C. Düllmann, T. Grahn, K. Hauschild, A. Herzán, R.-D. Herzberg, F. Heßberger, D. Hinde, R. Julin, S. Juutinen, E. Jäger, B. Kindler, J. Krier, M. Leino, B. Lommel, A. Lopez-Martens, D. Luong, M. Mallaburn, K. Nishio, J. Pakarinen, P. Papadakis, J. Partanen, P. Peura, P. Rähkila, K. Rezyunkina, P. Ruotsalainen, M. Sandzelius, J. Sarén, C. Scholey, J. Sorri, S. Stolze, B. Sulignano, C. Theisen, A. Ward, A. Yakushev, V. Yakusheva, *Phys. Lett. B* **764** (2017) 265 – 270. doi:http://dx.doi.org/10.1016/j.physletb.2016.11.038. URL [//www.sciencedirect.com/science/article/pii/S0370269316307018](http://www.sciencedirect.com/science/article/pii/S0370269316307018)
  - [3] V. I. Kuznetsov, N. K. Skobelev, G. N. Flerov, *Sov. J. Nucl. Phys.* **4** (1967) 202.
  - [4] V. I. Kuznetsov, N. K. Skobelev, G. N. Flerov, *Sov. J. Nucl. Phys.* **5** (1967) 271.
  - [5] H. L. Hall, K. E. Gregorich, R. A. Henderson, C. M. Gannett, R. B. Chadwick, J. D. Leyba, K. R. Czerwinski, B. Kadkhodayan, S. A. Kreek, N. J. Hannink, D. M. Lee, M. J. Nurmiä, D. C. Hoffman, C. E. A. Palmer, P. A. Baisden, *Phys. Rev. C* **42** (1990) 1480–1488. doi:10.1103/PhysRevC.42.1480.
  - [6] H. L. Hall, K. E. Gregorich, R. A. Henderson, C. M. Gannett, R. B. Chadwick, J. D. Leyba, K. R. Czerwinski, B. Kadkhodayan, S. A. Kreek, D. M. Lee, M. J. Nurmiä, D. C. Hoffman, C. E. A. Palmer, P. A. Baisden, *Phys. Rev. C* **41** (1990) 618–630. doi:10.1103/PhysRevC.41.618.
  - [7] D. Habs, H. Klewe-Nebenius, V. Metag, B. Neumann, H. J. Specht, *Z. Phys. A* **285** (1) (1978) 53–57. doi:10.1007/BF01410224.
  - [8] H. L. Hall, K. E. Gregorich, R. A. Henderson, C. M. Gannett, R. B. Chadwick, J. D. Leyba, K. R. Czerwinski, B. Kadkhodayan, S. A. Kreek, D. M. Lee, M. J. Nurmiä, D. C. Hoffman, *Phys. Rev. Lett.* **63** (1989) 2548–2550. doi:10.1103/PhysRevLett.63.2548.
  - [9] P. Möller, A. J. Sierk, T. Ichikawa, A. Iwamoto, R. Bengtsson, H. Uhrenholt, S. Åberg, *Phys. Rev. C* **79** (2009) 064304. doi:10.1103/PhysRevC.79.064304.
  - [10] P. Möller, A. J. Sierk, T. Ichikawa, A. Iwamoto, M. Mumpower, *Phys. Rev. C* **91** (2015) 024310. doi:10.1103/PhysRevC.91.024310.
  - [11] D. Kaji, K. Morimoto, H. Haba, E. Ideguchi, H. Koura, K. Morita, *J. Phys. Soc. Jpn.* **85** (1) (2016) 015002. doi:10.7566/JPSJ.85.015002.
  - [12] L. Ghys, A. N. Andreyev, S. Antalic, M. Huyse, P. Van Duppen, *Phys. Rev. C* **91** (2015) 044314. doi:10.1103/PhysRevC.91.044314.
  - [13] P. Möller, J. Nix, K.-L. Kratz, *Atom. Data Nucl. Data* **66** (2) (1997) 131 – 343. doi:http://dx.doi.org/10.1006/adnd.1997.0746.
  - [14] K. Morita, K. Morimoto, D. Kaji, H. Haba, E. Ideguchi, R. Kanungo, K. Katori, H. Koura, H. Kudo, T. Ohnishi, A. Ozawa, T. Suda, K. Sueki, I. Tanihata, H. Xu, A.V. Yeremin, A. Yoneda, A. Yoshida, Y.-L. Zhao, T. Zheng, *Eur. Phys. J. A* **21** (2) (2004) 257–263. doi:10.1140/epja/i2003-10205-1.
  - [15] F. G. Kondev, S. Lalkovski, *Nucl. Data Sheets* **112** (2011) 707.
  - [16] V. Kalinin, V. Dushin, F.-J. Hambsch, V. Jakovlev, K. Il'ya, A. Laptev, B. Petrov, G. Petrov, Y. Pleva, O. Shcherbakov, V. Sokolov, A. Vorobyev, *J. Nucl. Sci. Technol.* **39** (sup2) (2002) 250–253. doi:10.1080/00223131.2002.10875086.
  - [17] A. N. Andreyev, S. Antalic, D. Ackermann, L. Bianco, S. Franchoo, S. Heinz, F. P. Heßberger, S. Hofmann, M. Huyse, Z. Kalaninová, I. Kojouharov, B. Kindler, B. Lommel, R. Mann, K. Nishio, R. D. Page, J. J. Ressler, B. Streicher, S. Saro, B. Sulignano, P. Van Duppen, *Phys. Rev. C* **87** (2013) 014317. doi:10.1103/PhysRevC.87.014317.



- [18] S. Hofmann, D. Ackermann, S. Antalic, H. G. Burkhard, V. F. Comas, R. Dressler, Z. Gan, S. Heinz, J. A. Heredia, F. P. Heßberger, J. Khuyagbaatar, B. Kindler, I. Kojouharov, P. Kuusiniemi, M. Leino, B. Lommel, R. Mann, G. Münzenberg, K. Nishio, A. G. Popeko, S. Saro, H. J. Schött, B. Streicher, B. Sulignano, J. Uusitalo, M. Venhart, A. V. Yeremin, *Eur. Phys. J. A* 32 (3) (2007) 251–260. doi:[10.1140/epja/i2007-10373-x](https://doi.org/10.1140/epja/i2007-10373-x).
- [19] K. Nishio, S. Hofmann, F. P. Heßberger, D. Ackermann, S. Antalic, V. Comas, Z. Gan, S. Heinz, J. A. Heredia, H. Ikezoe, J. Khuyagbaatar, B. Kindler, I. Kojouharov, P. Kuusiniemi, B. Lommel, M. Mazzocco, S. Mitsuka, Y. Nagame, T. Ohtsuki, A. G. Popeko, S. Saro, H. J. Schött, B. Sulignano, A. Svirikhin, K. Tsukada, K. Tsuruta, A. V. Yeremin, *AIP Conf. Proc.* 891 (1) (2007) 71–79. doi:<http://dx.doi.org/10.1063/1.2713502>.
- [20] M. Takeyama, D. Kaji, K. Morimoto, Y. Wakabayashi, F. Tokanai, K. Morita, in: *Proceedings of International Symposium on Radiation Detectors and Their Uses* [in print], 2016.
- [21] V. E. Viola, K. Kwiatkowski, M. Walker, *Phys. Rev. C* 31 (1985) 1550.
- [22] D. C. Hoffman, *Nucl. Phys. A* 502 (1989) 21 – 40. doi:[http://dx.doi.org/10.1016/0375-9474\(89\)90652-0](http://dx.doi.org/10.1016/0375-9474(89)90652-0).
- [23] F.P. Heßberger, *Eur. Phys. J. A* 53, (2017) p.75.
- [24] P. Möller, J. Nix, W. Swiatecki, *Nucl. Phys. A* 492 (3) (1989) 349 – 387. doi:[http://dx.doi.org/10.1016/0375-9474\(89\)90403-X](http://dx.doi.org/10.1016/0375-9474(89)90403-X).
- [25] P. Cagarda *et al.*, In *Proc. 5th International Conference "Dynamical Aspects of Nuclear Fission"* (DANF), World Scientific Publishing Co. Pre. Ltd (2002) p.398
- [26] S. A. Kreek, H. L. Hall, K. E. Gregorich, R. A. Henderson, J. D. Leyba, K. R. Czerwinski, B. Kadkhodayan, M. P. Neu, C. D. Kacher, T. M. Hamilton, M. R. Lane, E. R. Sylwester, A. Türlér, D. M. Lee, M. J. Nurmiä, and D. C. Hoffman, *Phys. Rev. C* 50 (1994) p.2288.
- [27] P. Greenlees, P. Kuusiniemi, N. Amzal, A.N. Andreyev, P.A. Butler, K. Cann, J. Cocks, O. Dorvaux, T. Enqvist, P. Fallon, B. Gall, M. Guttormsen, D. Hawcroft, K. Helariutta, F.P. Heßberger, F. Hoellinger, G. Jones, P. Jones, R. Julin, S. Juutinen, H. Kankaanpää, H. Kettunen, M. Leino, S. Messelt, M. Muikku, S. Ødegård, R. Page, A. Savelius, A. Schiller, S. Siem, W. Trzaska, T. Tveter, J. Uusitalo, *Eur. Phys. J. A* 6 (3) (1999) 269–273. doi:[10.1007/s100500050345](https://doi.org/10.1007/s100500050345).
- [28] A. N. Andreyev, D. D. Bogdanov, V. I. Chepigin, A. P. Kabachenko, S. Sharov, G. M. Ter-Akopian, A. V. Yeremin, O. N. Malyshev, *Z Phys. A* 337 (2) (1990) 231–232. doi:[10.1007/BF01294297](https://doi.org/10.1007/BF01294297).
- [29] W. Reisdorf, *Z. Phys. A* 300 (2) (1981) 227–238. doi:[10.1007/BF01412298](https://doi.org/10.1007/BF01412298).
- [30] M. Asai, M. Sakama, K. Tsukada, S. Ichikawa, H. Haba, I. Nishinaka, Y. Nagame, S. Goto, Y. Kojima, Y. Oura, H. Nakahara, M. Shibata, K. Kawade, *Eur. Phys. J. A* 23 (3) (2004) 395–400. doi:[10.1140/epja/i2004-10096-6](https://doi.org/10.1140/epja/i2004-10096-6).
- [31] M. Sakama, M. Asai, K. Tsukada, S. Ichikawa, I. Nishinaka, Y. Nagame, H. Haba, S. Goto, M. Shibata, K. Kawade, Y. Kojima, Y. Oura, M. Ebihara, H. Nakahara, *Phys. Rev. C* 69 (2004) 014308. doi:[10.1103/PhysRevC.69.014308](https://doi.org/10.1103/PhysRevC.69.014308).
- [32] M. Asai *et al.*, Private communication.